CRASHWORTHINESS OF COMPOSITE AIRCRAFT STRUCTURES

G. Labeas
Laboratory of Technology and Strength of Materials
Department of Mechanical Engineering & Aeronautics
University of Patras
Patras 26500, Greece

OVERVIEW

The forthcoming text reflects a selection of research findings in the area of impact and crashworthiness of composite aircraft components, which have been analysed by the author in the frame of the European Research Projects 'Design for Crash Survivability - CRASURV', 'Crashworthiness of aircraft for high velocity impact – CRAHVI' and "Cellular Structures for Impact Performance - CELPACT", (refs. [23], [24] and [25]). The author wish to acknowledge financial support from CEC under the FP5 and FP6 Research Programmes.

1. INTRODUCTION

The present paper discuses current research issues of crashworthiness design and impact simulation of composite structures. The crashworthiness requirements and characteristics, the failure behavior of composite structures in crash conditions and the modeling strategies using non-linear dynamic numerical codes are considered. Various energy absorbing composite elements are analysed in detail and their failure behavior is numerically simulated.
The main goal of crashworthiness is to maintain the structural integrity of the aircraft in order to provide the highest probability of occupant survival. Towards this target, three main aspects are considered in the present paper.
The first aspect deals with the introduction of energy absorption capabilities in a composite fuselage construction and refers to low-velocity impact. Some of the principles for providing composite design concepts towards the maximum crash survivability of the occupants are described. The energy absorption element considered in detail is the 'tensor skin concept', comprising folded composite layers, which unfold under the impact load and increase the energy absorption capability of the structure. A numerical simulation procedure, verified by experimental work, is applied in the process of development the 'tensor skin concept' for the lower fuselage structure.
The second aspect deals with the novel design of a fibre-reinforced composite Leading Edge (LE) and refers to bird-strike protection. The design concept is based on the absorption of the major portion of the bird kinetic energy by the composite skins, in order to protect the ribs and the inner LE structure from damaging. A numerical model simulating the bird strike process is developed and verified by bird strike experimental tests. The influence of the critical modelling issues in the numerical results, such as, the mesh density of the highly impacted areas, the substitute bird flexibility, as well as, the material damage and contact interfaces parameters are discussed in detail.
The third aspect deals with the introduction of cellular materials in the crashworthiness design. Cellular structures are sandwich structures characterized by the construction of their core, which is made of an interconnected network of solid struts or shell-type shapes. Focus on the failure behaviour of metallic open lattice cellular cores, which is considered to be one of the keys to the successful development of improved sandwich structures with tailored properties, is currently performed. The failure behaviour is analysed by means of numerical simulation and Finite Element modelling of cellular cores. Buckling analysis is used to identify the buckling load and buckling mode of the structures, as well as, to calculate the artificial imperfections to be introduced in a consequent non-linear elastoplastic analysis. The latter is used to predict the failure load and mode of the sandwich structures.

2. ENERGY ABSORPTION CAPABILITIES OF COMPOSITE FUSELAGE CONSTRUCTION FOR LOW-VELOCITY IMPACT

Crash survival requires that both the vehicle and the occupant survive the impact, so that the occupant is able to evacuate the plane before any post-crash environment hazards, such as fire or water become intolerable [1]. Amongst the successive requirements that should be fulfilled towards this target, the maintenance of the occupant living space has the first priority, implying a crashworthiness design of the structure.
The energy absorption capability of the ordinary composite structures under impact loading is usually low, due to the limited ability of composite materials to absorb impact energy [2]. To enable crashworthiness in aircraft and helicopter fuselage structures, special design of their subfloor boxes is required. Examples of crashworthiness subcomponents are the different geometrical configurations of box-beams, sinewave beams, sandwich panels and cruciforms [3, 4].
Following the above concept for developing energy absorbing composite structures, the 'tensor skin' panel has been recently introduced. The 'tensor skin' panel combines the capabilities of high energy absorbing composite material with an energy absorbing design philosophy. It has been originally developed to improve the water impact crashworthiness of helicopters with fuselage structure made of composite materials [5, 6]. The 'strain to failure' limits of the 'tensor skin' material system are much higher than the common 1% to 2% of

the ordinary composite material systems. Furthermore, experimental tests have shown than the energy absorption mechanism of the unfolding 'tensor skin' strip is quite effective [7]. When this strip is loaded in tension or bending, the beam unfolds and deflects by forming 'plastic hinges' before it stretches and fails in tension. The fact that the final failure is dictated by the strength of fibers leads to an increase of the load bearing capability of the structure. Therefore, it is expected that utilization of 'tensor skins' in the susceptible to impact areas of a helicopter or airplane subfloor structure will allow the absorption of a satisfactory amount of impact energy.
The development of 'tensor skins' strongly requires extensive experimental testing in order to verify the energy absorption capabilities of the developed components. However, tooling, manufacturing and testing of components are quite expensive. To allow parameter studies and minimize the tests, prediction techniques for crash behaviour of composite structures are required. The widely applied Finite Element (FE) method is a suitable tool for the modeling and the simulation of the initiation and propagation of different types of failure within an impacted structure [3]. However, less reliability exists in the utilization of such codes in the case of composite structures as compared to the metallic ones. Major issues of the numerical simulation of composite structures under impact are the proper representation of the composite material behaviour, the prediction of the complex failure modes and the development of adequate FE meshes, which will lead to accurate results in reasonable solution times.
In the present work the non-linear dynamic FE code, PAM-CRASH [8] is used in the numerical simulations. The simulated experimental tests are quasi-static crush tests of three-dimensional 'tensor skin' panels. The main issues of the simulation methodology are described in detail. The simulation results are generally in good agreement to the experimental ones. It is concluded that the investigated structures may be successfully applied in the absorption of the impact loads.

2.1. Numerical analysis methodology and material model

In PAM-CRASH code, a unidirectional fibre or fabric reinforced composite ply, may be modeled as a homogeneous orthotropic elastic or elastic- plastic damaging material, having properties that are degraded on loading by microcracking, prior to ultimate failure. A Continuous Damage Mechanics formulation is used, in which ply degradation parameters are internal state variables, governed by damage evolution equations. Constitutive laws for orthotropic elastic materials with internal damage are described in [9] and have the general form:

(1) $\boldsymbol{\varepsilon}^e = \mathbf{S}\boldsymbol{\sigma}$

where, $\boldsymbol{\sigma}$ and $\boldsymbol{\varepsilon}^e$ are vectors of stress and elastic strain and $\mathbf{S}$ the elastic compliance matrix. For shell elements a plane stress formulation with orthotropic symmetry axes is used. The in-plane stress and strain components are:

(2) $\boldsymbol{\sigma} = (\sigma_{11},\ \sigma_{22},\ \sigma_{12})^T$

(3) $\boldsymbol{\varepsilon}^e = (\varepsilon^e_{11},\ \varepsilon^e_{22},\ \varepsilon^e_{12})^T$

The ply damage model implements three scalar damage parameters d_i, d_1, d_u, which in general, take values between zero and unity and represent modulus reductions under different loading conditions, due to microdamage in the material. The initial undamaged inplane stiffness properties E_{11}, E_{22}, G_{12} and v_{12} define the initial modulus matrix $\mathbf{C}_0$ of each layer. The damage function d enables the representation of the degradation of the initial modulus matrix $\mathbf{C}_0$ when the deformation level that the material damage initiates has been exceeded. The modulus matrix, thus, behaves according to the formulae:

(4) $\mathbf{C}(d) = \mathbf{C}_0(1-d)$

The damage function is a scalar parameter that depends upon strain (ε) as:

(5) $d(\varepsilon) = d_v(\varepsilon_v) + d_s(\varepsilon_s)$

where, d_v is the volumetric damage due to a volumetric equivalent strain ε_v and d_s is the shear damage parameter due to a shear equivalent strain ε_s. The scalar parameter ε_v represents the first invariant of the volumetric strain tensor, while the scalar ε_s represents the second invariant of the deviatoric strain tensor. The implemented damage law in PAM-CRASH assumes that the fracturing damage parameter d is zero for an equivalent strain between zero and ε_i (FIG 1-i). After the value ε_i is reached, the fracturing damage factor d grows linearly between the values ε_i and ε_1. Between ε_1 and ε_u the damage factor d grows linearly again, with a different slope. The damage parameters corresponding to the strains ε_i, ε_1 and ε_u are d_i, d_1 and d_u, respectively, where d_u is the stage where the ultimate damage is reached. The elasticity modulus is assumed to degrade according to FIG 1-ii and is related to uniaxial data according to FIG 1-iii.
The application of the PAM-CRASH material damage modeling technique to develop and calibrate suitable material damage models, which properly describe the elastic properties degradation, as well as, the damage initiation and propagation, is very critical for the success of the simulation.
The 'tensor skin' structures, studied in present, comprise unidirectional and fabric 'Dyneema' plies. The calibration of material damage models for the unidirectional plies of composite laminates can be performed either by using the experimental tension-compression stress-strain curves translated to volumetric damage only, or by using the experimental shear stress-strain curves translated to shear damage only. In both cases, the developed material model leads to a successful simulation of the structure behaviour. However, the calibration of material damage models for the fabric composite plies is more difficult. In present, the experimental material data of ref. [10] and [11] are used to calibrate the 'Dyneema' fabric plies. It is concluded that, for fabric plies, if the material damage model is based either only on volumetric, or only on shear damage, the experimental tension/compression behaviour can be successfully represented. This is not the case for the shear behaviour, which is overestimated or underestimated, respectively, if only volumetric or only shear damage modeling parameters are used. On the other hand, when for the material

model calibration, only shear experimental curves are used, an enormous overestimation of the tension/compression strengths is observed in the model behaviour. This happens due to the fact that the composite fabrics have a completely different behavior in tension/compression (ε_{max} is between 1% and 3%) and shear (γ_{max} is between 10% and 25%). For a successful representation of the global behaviour of composite fabrics, the damage models in the present work are calibrated starting with the calculation of the shear damage from coupon shear tests, while the volumetric damage parameters are introduced afterwards, only for the cut-off the final residual strength in order to match the tension/compression data.

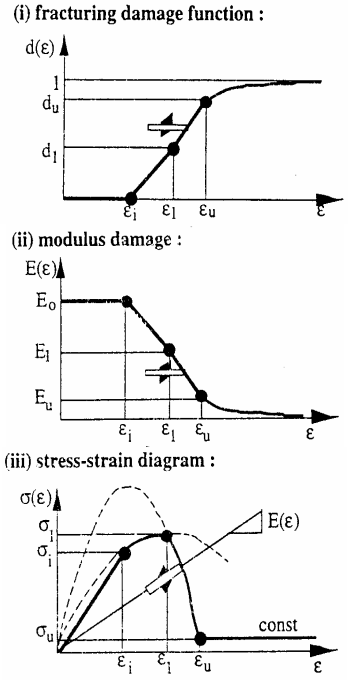

FIG 1. Fracturing damage function, modulus degradation and stress-strain diagram, [8].

2.2. Crushing simulation of three-dimensional tensor skin panels

The three-dimensional 'tensor skin' panel, shown in FIG 2a, is a practical realization of the 'tensor skin' concept. It is a sandwich panel comprising a corrugated skin surrounded by an inner (hat shaped) and an outer face. The material systems utilized for the inner and outer facings are Carbon-Aramid/epoxy hybrid fabric (trade name Hexcel 73210-2-1220-F155-45%) and Aramid/epoxy fabric (Hexcel F-155-49-285-52%), respectively. The corrugated core of the panel is made of 'Dyneema' layers. Experimental data from tension, compression and shear coupon tests for these materials are taken from ref. [12] and [13]. The 'tensor skin' sandwich panel has dimensions 540x540mm and its cross section is shown in FIG 2b.

In order to estimate the energy absorption capability of the sandwich system, A FE model of the 3-D panel is developed in the present work for the numerical simulation of the experimental tests of ref. [14]. Geometrical and material data for the modeling have been taken from [15] and the material damage calibration methodology described above is applied. The FE mesh, shown in FIG 3, comprises 5400 elements (3837 nodes) and is typical of the FE models developed for the simulation of the 3-D panel. For the representation of the connectivity between the three panel faces, a tied contact algorithm, coded in PAM-CRASH as contact 'type 2', is utilized. The contact algorithm requires input of normal N_s and shear T_s strengths of the tied interface and enables the contact failure, after the contact force of the tied nodes is exceeded. Failure is assumed to occur when:

$$(6)\quad \left(\frac{N}{N_s}\right)^2+\left(\frac{T}{T_s}\right)^2 \geq 1$$

Both the normal N_s and shear T_s strengths of the tied interfaces are assumed to be 5KN. These values were estimated from the mechanical properties of the bond (Argomet F13) and the average area of the elements of the FE mesh. The calculation of these strength values is a very critical point of the analysis [17]. The strength values determine the introduction of one of the basic failure modes of the system, i.e. the debonding of the three different layers of the panel. If the debonding occurs early, then all the load is carried by the layers individually, which means that the total bending stiffness is seriously reduced, resulting to a pre-mature collapse of the whole system.

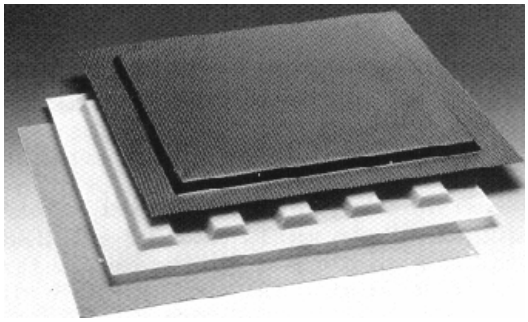

(a)

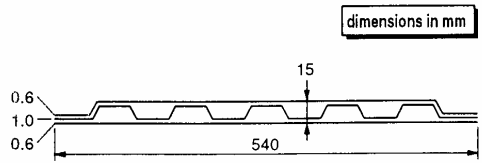

(b)

FIG 2. (a)The 3-D 'tensor skin' panel' and (b) Cross section of the corrugated 3-D 'tensor skin' panel, after [14]

For the modeling of the contact between the structure interfaces, the self-contact algorithm, coded in PAM-CRASH as contact 'type 26' is applied. This contact algorithm automatically searches for elements contacting each other and introduces an internal contact force between these elements.

The calculated deformed shapes of the outer (left), middle (center) and inner (right) faces, of the panel with a corrugated core laminated at $[\pm 45]_3$, at various time intervals are shown in FIG 3. The calculated rigid wall force versus the rigid wall displacement is shown in FIG 4. By observation of the inner and outer faces of the panel in FIG 3, it can be observed that both faces start failing at about the simulation interval of t=0.39ms, which corresponds to a rigid wall force of 36KN and

rigid wall displacement 39mm. Again from FIG 3, it arises that the time for the final Dyneema failure is 0.83ms, which corresponds at rigid wall force of 149KN and rigid wall displacement of 178mm (FIG 4 and FIG 5). In FIG 5 the measured tool force versus tool displacement is plotted, after [14]. The first sharp drop in the diagram (tool force of 31.8KN and rigid wall displacement of 42mm) corresponds to the outer and inner faces failure, while the second sharp drop (tool force of 171KN and rigid wall displacement 149mm) implies the final failure of the Dyneema layers. Comparing FIG 4 to the experimental results of ref. [14] a very good agreement is observed between the calculated and measured tool force and displacement histories, especially concerning the peak loads, which are critical points of the analysis.

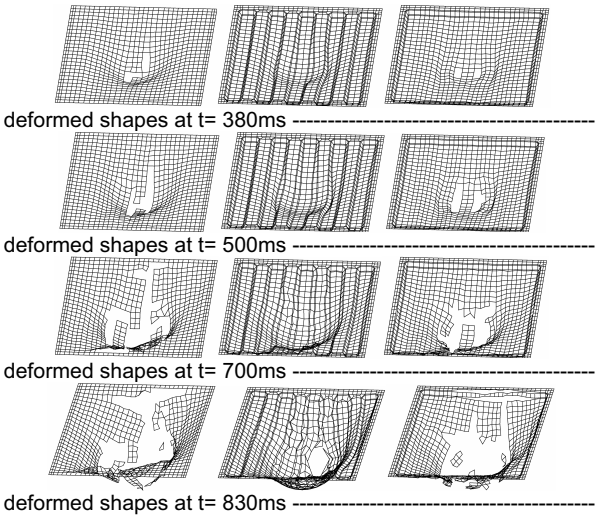

FIG 3. Deformed shapes of the outer (left), middle (center) and inner (right) faces, at various time intervals, of the static crush test of a 3-D 'tensor skin' panel.

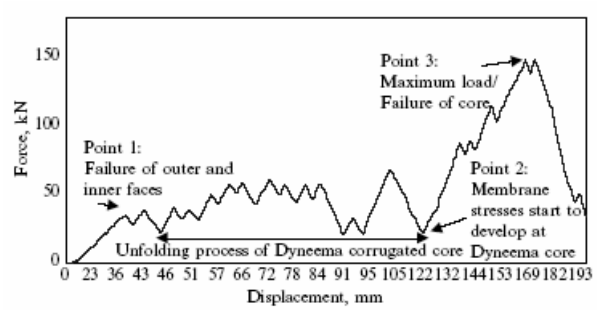

FIG 4. Rigid wall force vs. displacement of the static crush test of a 3-D 'tensor skin' panel.

3. NOVEL DESIGN OF A FIBRE-REINFORCED COMPOSITE LEADING EDGE (LE) FOR BIRD-STRIKE

The Leading Edge is the front edge of a main wing, horizontal or vertical stabilizer and has several important functions during flight, most important of which are the aerodynamic function and the offering of space to high lift devices (flaps, slots, slats, drooped nose) and ice protection systems. In the same time, the LE should fulfil the critical safety requirement to protect the wing torsion box and control devices from any significant damage that may occur, such that the aircraft can land safely; therefore the LE should be designed for bird strike resistance. For the HTP considered in the current study design requirements state that the bird strike load acting anywhere on the LE skin must not exceed 200 kN to avoid excessive loads on the stabilizer brackets. Furthermore, a design solution in which the complete bird kinetic energy can be absorbed by the Leading Edge alone is required; otherwise, the bird approaches the brittle composite front spar, which is not usually capable of absorbing energy. The available space within the leading edge is relatively small regarding the amount of kinetic energy and the poor energy absorption capabilities of transversely loaded composite structures. Consequently, a Leading Edge comprising a highly efficient composite energy absorbing structure must be developed to accomplish the above requirements and decelerate the bird in a control motion until it completely stops before reaching the wing front spar.

The 'tensor skin' concept, which is developed for energy absorption of transversely loaded composite structures within a limited space, is applied for the novel design of the composite LE. A complete LE tensor skin structure is developed and simulations of dynamically bird strike resistance tests are performed.

The capability of simulating the complex failure modes of the novel composite LE structure is very important for the design process, as it allows to study the effect of the design variables on the energy absorption characteristics, to assess the scaling effects between full-scale behaviour and tested models and thus to minimize the testing effort. The development of the simulation methodology is described in detail and the numerical parameters affecting the computed values are studied. It is concluded that the simulation results are in good agreement to the experimental ones, therefore, the numerical approach can be considered as an important supporting tool in the design and proof process of innovative crashworthiness concepts.

3.1. Description of energy-absorbing tensor skin concept

The skin configuration of the novel composite LE design comprises three groups of plies, namely the 'carrying', 'tensor' and 'cover' plies, as schematically presented in FIG 5, which have different functionalities. The load carrying plies transfer the normal operational aerodynamic load to the ribs, therefore they provide the usual LE skin stiffness. The second group of plies, the tensor plies, contain folded loops between the ribs, which are to unfold when a relatively high lateral load is applied to the skin, e.g. in the case of bird strike. Under normal flight conditions the tensor plies are without any function. In case of a relatively high lateral load all plies except the tensor plies fail. Under the induced penetration load, the tensor plies start unfolding, acting as plastic hinges, until they are loaded in tension like a membrane. Fibres of the composite fabric material unfold from their loop and are loaded in a way comparable to a hammock. When the tensor plies are

completely unfolded, the vertical load component is transferred to the ribs as compressive load. The third group of plies has the purpose to cover the tensor skin. The skin to rib attachment is realized with fasteners conforming to common aviation types of attachment.

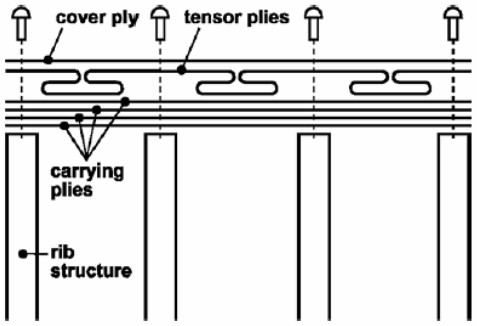

FIG 5. Schematic representation of the LE structural configuration, after [23].

3.2. Validation of the novel composite Leading Edge design

For the validation of the novel LE design, the capability of the structure to meet the design requirements should be tested through dynamic bird strike tests. The non-linear finite element code PAM-CRASH [8] is used for the numerical simulations of the bird-strike tests.

LE dimensions	Sub-laminate	Lay-up	Laminate ID	Remarks
rib-pitch: 230 mm length: 850 mm	Dyneema SK65 fabric with AF163-2K	$[0_3,45,0_3]$	Tensor	**Note:** Adhesive film between the 3 tensor sub-laminates only at the rib areas.
	Carbon/Aramid hybrid prepreg	[45, 0, 90, 0, 45]	Carrying	
	Aramid/epoxy prepreg	[0]	Cover	
	Aramid/epoxy prepreg	$[45]_2$	Protection-strip (40 mm)	

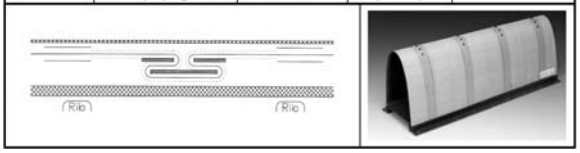

TAB 1. Design and lay-up of the Leading Edge structure, after [23]

The LE structure designed and fabricated for the full LE bird strike test is presented in TAB 1, including the information on the composite skin sub-laminates lay up and the LE overall dimensions. The full LE bird strike test has been carried out under the approximated real bird impact conditions, as presented in ref. [18]. The substitute bird had a mass of 4 lbs (1.81 kg), density close to the real bird density and impact behaviour close to the one observed in real bird impacts, i.e. flowing over the structure and spreading the impact load over a significant surface area. The substitute bird impactor is made of gelatine, as it has the closest possible physical properties to the living birds. The gelatine density is 950 kg/m3, which is close to the real bird density. The geometry of the substitute bird impactor approximates well enough the shape and dimensions of the real bird body. The results of the numerical simulation of bird strike on the tensor skin LE structure are presented in section 3.2.2

3.2.1. A study of the bird strike simulation modelling parameters

The numerical model development process comprises two phases; the initial stage where the model parameters are roughly set in order to asses the general model efficiency and the model enhancement phase, in which the sensitivity of the model parameters is studied by comparison between the simulation results and bird-strike experimental results, in order to optimize the FE model. This study demonstrated that the most critical modelling parameters are: the FE mesh element size (mesh density at the impacted area), the contact interface thickness and the parameters of the bird impactor model. Of major influence is also proven to be the material model applied. The material model for fabric composite materials in PAM-CRASH FE code has been described in section 2.1. Due to the parameters cross-influence, assessing the optimal set required numerous runs and thorough examination of each parameter affecting the numerical results.

The novel LE structure is initially modelled by a relatively rough FE mesh, of average element size of 20 mm, comprising a total of 12 888 shell elements with no mesh refinement in the highly loaded impacted areas. This initial FE mesh is considered acceptable for ordinary stress analysis purposes in large-scale models. The FE model consists of the sub-models of the LE-cover laminate, the LE-tensor laminate, the LE-carrying laminate, as well as, models of the four ribs and their protection strips. Comparisons of bird strike simulations using this initial mesh, to bird strike experimental results have shown very poor deformability of the composite LE skins. Following the idea that increasing the mesh density in the highly loaded areas of the LE will increase the skin deformability and allow for the reduction of the contact interface stiffness (explained in the following section 3.2.1b), the FE mesh is refined in the area between the mid ribs where the bird impacts the structure. The average element size in this area is set to 5 mm resulting to a total number of 28 638 shell elements for the enhanced model. The mesh refinement has contributed significantly in assessing the desired deformability of the LE skin, although resulted to an increase of the required calculation time

The physical or fixed contact between the LE components is numerically modelled by introducing contact interfaces in the model. In general, the number of the defined contact interfaces should be kept as small as possible, due to their big influence on the increase of the calculation time. However, due to the complex geometry of the tensor skin layers, introduction of numerous contact definitions is necessary in the area of the impact. Three different types of contact algorithms are used:

a) The enhanced tied interface with failure is used to model the adhesive film tying the LE facings to each other and the fixing of the LE skin to the ribs. The search algorithm of this contact type creates a search box around a master segment of height hcont, as shown in FIG 11, and in all the nodes found in this box an internal force depending on the relative stiffness of

the contacting elements is applied. The default value of the contact thickness hcont is calculated as [8]:

(7) $h_{cont} = 0.2\sqrt{A/8}$

where, A is the element surface area of the master segment. This contact type can be deactivated if the interface force grows over the limit force, called the rupture force. The definition of the rupture force is given by the equation (6), and for the case of novel LE design model the normal N_s and shear T_s strengths of the tied interface are defined to be 5,1KN and 3,2KN respectively, and coefficients a and b are set to 1.5 and 2.1, respectively.
The contact thickness for tied contacts is set to 5 mm, all over the refined FE model. A smaller contact thickness would not activate the contact between the layers, as the shell elements of the individual facings are placed in the mid-plane of the facings. A higher contact thickness has caused interference problems between the contact definitions, since the tensor skin comprises a total of six successive groups of plies, as shown in FIG 1.

b) The node to surface interface is used for modelling of the physical contact between the bird impactor and the LE skin; the LE skin is determined as the master segment and the impactor nodes as the slave nodes. The contact thickness is set to 10 mm, equal to the average element size of the entire FE mesh.

c) The self-impacting interface with edge treatment is applied to model the physical self-contact between LE sub-laminates in the regions where no adhesive film is applied. The parametric study, in which the contact thickness has been varied between 1mm and 10mm, has resulted to the optimum contact thickness of 3 mm for the current structure. The definition of such a low contact thickness value has become possible after the mesh refinement of the LE skin at the mid ribs area and the reduction of the element size, which resulted to the decrease of the stiffness of the contact interfaces and has led to more realistic deformability of the structure.

d) Substitute bird model

The proper numerical modelling of the substitute bird requires a material damage model for the soft gelatine material and a technique to overcome the numerical errors that occur due to the large FE mesh distortions that take place during the high velocity impact. The Smooth Particle Hydrodynamic (SPH) method is adopted in present. SPH is a gridless computational method whose foundations are in the interpolation theory. The material is represented as a set of discrete particles (interpolation points), which are topologically independent from each other and are combined through the material law of a 'hydrodynamic solid'. A kernel function is assigned to the SPH model that defines a range of influence of a particle in the continuum. Each particle has an associated mass, velocity and stress state, which evolves according to the discretized field equations. Contact laws between particles and conventional finite elements are introduced, so that it is possible to combine an SPH impactor model to a FE structural model. The Murnaghan equation of state is used to model the gelatine material [8]:

(8) $p = p_0 + B\,[(\rho/\rho_0)\gamma - 1]$

where, p_0 is the initial pressure in the material, B is the gelatine bulk modulus, γ is gamma exponent having the value of 7 and ρ/ρ_0 is the ratio of the mass density at a deformed state over the initial mass density of the undeformed state. The intensity of the cross-influence of the solid nodes (smooth particles) of the SPH model is controlled by the anti-crossing force parameter, which affects the 'independency' of the solid nodes, thus the deformability of the SPH model. The default value of this parameter is zero implying a completely independent behaviour, however in most cases this value causes numerical errors during the simulation. A parametric study was performed, ranging this parameter between the zero value and 0.1. The value 0.001 has been found to be optimal for the present bird strike simulations, as higher values resulted to large deformations of the LE, unrealistic in comparison with the test, while values below 0.001 are causing numerical errors during the simulation.

3.2.2. Results of bird strike simulation on the tensor skin LE structure

The FE model of the bird strike test is presented in FIG 6. It may be observed that the test rig has been included in the model, in order to enable the calculation of the reaction forces. A comparison of the bird strike sequence captured in the test in comparison to the respective simulation is shown in FIG 7. It may be observed that in the test, the impactor perforated the Leading Edge skin, leaving a hole in the area of impact. Some of the impactor material penetrated deeper into the LE, representing a potential danger for the inner Leading Edge components. According to the simulation, the opening occurs initially on the cover laminate, at the mid length of the LE and spreads along the entire LE section. Observing the simulation sequence from different angles and sections, no unfolding of the Dyneema tensor skin has been noticed. Instead, the tearing of the tensor skin material occurred on the folded edges of the tensor loops, which is proven to be in agreement with the results from the examination of the LE skin after the bird strike test. The simulation predicts well the experimental observations, regarding the deformation of the LE skin and penetration of the substitute bird material into the leading edge structure.

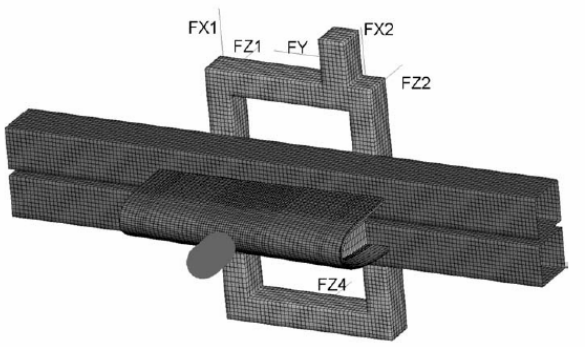

FIG 6. FE model of the full Leading Edge structure, including the bird impactor and the test rig.

The measured load cell response is reflected well in the simulation results, as can be noticed from FIG 10. It may be observed in the experimentally measured data, that the main reaction forces occur in the z-direction, which is the direction of the bird impact. The characteristic calculated response for all three forces FZ1, FZ2 and FZ4 (see FIG 6 for definitions) comprises an initial negative peak, followed by a positive peak force value and a fast stabilization of the force magnitude. The calculated forces in z-direction have a small phase difference with respect to the main oscillation modes of the experiment. Possible causes for this difference are the high elastic modules used in the simulation of the test rig components. From a comparison of the diagrams of FIG 8 it is also observed that the numerical model has higher damping, since the stabilization of the calculated forces is faster than in the experiment. The other reaction forces (in x and y direction) are much smaller and have no importance for the validation procedure.

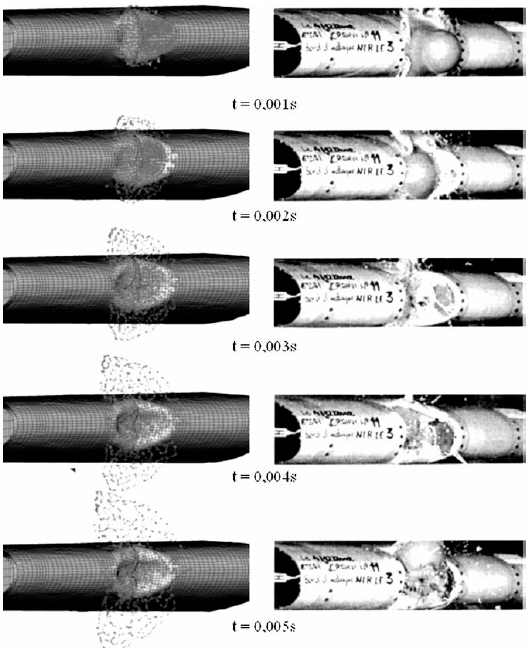

FIG 7. Bird strike sequence: simulation (left) and experiment (right).

4. CELLULAR STRUCTURES

Cellular structures are sandwich structures characterized by the construction of their core, which is made of an interconnected network of solid struts or shell-type shapes. The applications of cellular structures are widespread. Thermal insulation, packaging, structural, buoyancy and many other engineering sectors are the most common fields for the utilization of cellular structures [19]. The usual design parameters of cellular sandwich structures are the relative density, the elastic specific stiffness and strength [20]. The mechanical behaviour of sandwich structures is dependent on the mechanical properties of both core and composite skin. The cellular core behaviour is dependent on the cell geometry and cell size. The present work focuses on the failure behaviour of metallic open lattice cellular cores. This behaviour is considered to be one of the keys to the successful development of improved sandwich structures with tailored properties. The failure behaviour is analysed by means of numerical simulation via Finite Element modelling of cellular cores. Due to the high difference of size scale between the cell structure (which is usually of the order of a few millimetres) and the entire sandwich cellular structure, the ordinary numerical analysis methodologies lead to very large models, requiring high computing power for their solution. In contrary, alternative and multiscale modelling strategies are preferable. They are based on very detailed unit cell models using material properties, cell geometry and cell size for determining the cellular metallic core properties.

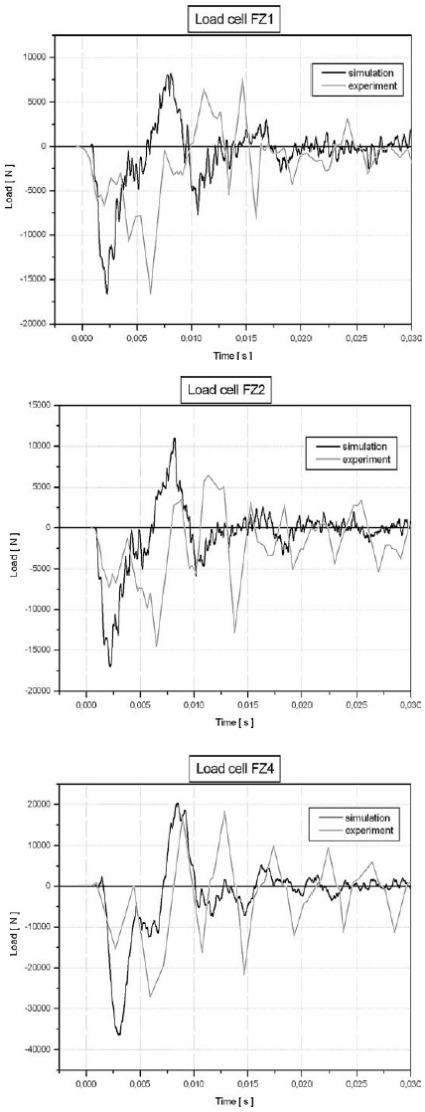

FIG 8. Comparison between simulated and measured forces on test rig load cell.

Three types of cellular cores, based on different unit cell configurations, namely, '*bcc*', '*bcc,z*' and 'f_2*fcc,z*' are investigated. The compression behaviour of the three types of cellular structures is simulated by adequate beam-type Finite Element models. The numerical analysis comprises a linear eigenvalue buckling analysis followed by a non-linear elastoplastic static analysis. The buckling analysis is used to identify the buckling load and buckling modes of the structures, as well as, to calculate the artificial imperfections to be introduced in the non-linear elastoplastic analysis. The latter is used to predict the failure load and mode of the structures. A strong effect of the radius of the unit cell struts and the unit cell size on the computed elasticity modulus and failure load is observed. Therefore, numerical results for varying strut radius and unit cell size are presented. It may be concluded that, if the detailed geometrical description of the unit cell structure is known and material properties at the size scale of the struts are provided, then the sufficiently accurate prediction of the cellular structure response is possible.

4.1. Numerical model description

The numerical simulations of the cellular structure deal with predicting the elasticity modulus and failure load of the structure in uniaxial compression. The numerical study is performed to analyze the effect of different arrangement of strut members inside the cell, as well as, the cell size and strut radius on the structure's elasticity modulus.
The cellular structure modelling and simulations refer to the cellular structures developed and tested in [21]. The cubic structures of dimensions 25x25x25 mm3 involve three different cell geometries, as presented in FIG 9, namely the 'bcc' cell with density of 994kg/m3, the 'bcc,z' cell having a higher density of 1258kg/m3, and the 'f2fcc,z' geometry with density of 983kg/m3. The unit cell structure is constructed using the selective laser melting technique with Stainless steel 316L as powder material [22]. The mechanical properties of this material are the modulus of elasticity equal to 193 GPa and the density equal to 8000 kg/m^3.
The beam element type BEAM188 is used in ANSYS finite element code [16] to model the unit cell. It is a three-dimensional beam element with six degrees of freedom per node, ideally applicable to problems involving geometrical non-linearity and plasticity. The FE refinement level in the present case studies varies from 1 to 4 elements per strut-member. Two surfaces of the structure that are perpendicular to the loading direction are selected for applying the compressive load and boundary conditions, as shown in FIG 12a. The load is applied as axial force on the nodes of the loading surface. The rigid movement of the loaded surface is achieved by applying coupled displacement in loading direction on all nodes of the loaded surface. On the opposite surface one corner node is selected to be constrained for translation in all directions, while for the remaining nodes only the translation in the loading direction is constrained, thus enabling the lateral displacement of the structure. A linear static numerical analysis is initially executed for predicting the elasticity modulus of the cellular structure. Consequently, a non-linear static analysis including geometrical and material non-linearity is performed to predict the failure load of the analyzed component; where required artificial imperfections are introduced by means of an eigenvalue buckling analysis.

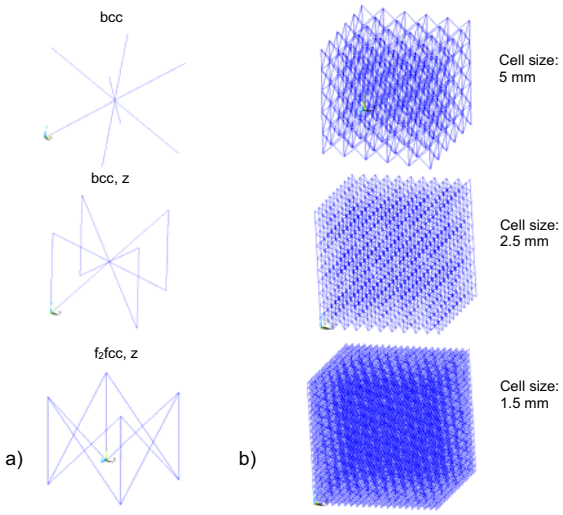

FIG 9. a) The three investigated unit cells types and b) Cellular core structures of 25x25x25 mm3 with cell sizes of 5mm, 2.5mm and 1.25mm

4.2. Prediction of elasticity modulus of the cellular structure

The elasticity modulus of a cellular structure depends directly on the unit cell geometry and size, strut radius and material properties. The current study focuses on the effect of the cell geometry on the elasticity modulus of the structure. For simple two-dimensional or three-dimensional geometries it is possible to calculate theoretically the elasticity modulus of the unit cell or the cellular structure by using the elementary mechanics of materials theory [19]. Applying the compressive axial load and assuming linear elastic static analysis, the elasticity modulus is estimated as the ratio of computed 'global' axial stress over the 'global' axial strain. The 'global' axial stress is calculated as the overall axial load over the loading surface (FIG 10a). The 'global' axial strain is calculated as the axial displacement of the loaded surface over the initial height of the structure (FIG 10b).

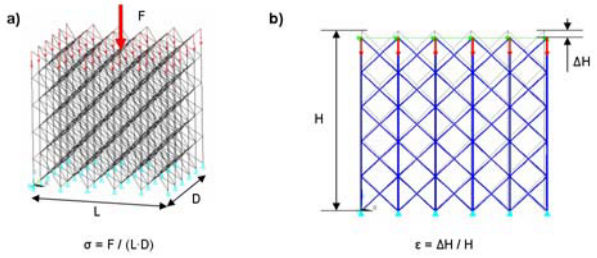

FIG 10. a) Calculation of the 'global' axial stress, and b) Calculation of the 'global' axial strain

The calculated elasticity moduli are compared to the measured values from [21] in TAB 2. It can be observed from both the experimental measurements and

calculated values that a variation of the unit cell geometry or size results to a radical change in the structure's elasticity modulus. As observed from TAB 2, the elastic moduli of the structures with bcc cell type are lower compared to that of structures with bcc,z and f2fcc,z cell type; this can be explained by the existence of additional axial members in the direction of loading in the bcc,z and f2fcc,z cells. Furthermore, an increase in the unit cell size decreases the structure stiffness and the respective elasticity modulus, which can be explained by observing that, as the cell size decreases, the effective loaded area tends to the value L x D (see FIG 10a) and the elasticity modulus of the structure tends to approach the bulk material elasticity modulus.

Cell type	*Measured average cross-section radius*	*Estimated cross-section radius*	*Cell size*	*Elasticity modulus experimental (GPa)*	*Elasticity modulus numerical (GPa)*
bcc	r=0,16mm	r=0,124mm	1,5 mm	0,44	0,42
		r=0,124mm	2,5 mm	0,05	0,051
bcc,z		r=0,08mm	1,5 mm	2,7	2,67
		r=0,06mm	2,5 mm	0,45	0,48
$f_2$fcc,z		r=0,08mm	1,5 mm	1,9	2,02
		r=0,09mm	2,5 mm	1	0,988

TAB 2. Measured and predicted elasticity moduli for different cell geometries and sizes

4.3. Failure of cellular structures in axial compression loading

The aim of the simulation of failure of cellular structures in axial compression loading is the estimation of the usual design parameters of cellular sandwich structures, which are the relative density, the elastic specific stiffness E_1, peak failure stress σ_{peak}, plateau strength $\sigma_{plateau}$, and compaction strain $\varepsilon_{compact}$ (FIG 11). Compaction strain is the strain value at which the stacking of the material layers finishes and the load is transferred by the contact between the layers of stacked beams. A simple engineering approach is used for estimation of the compaction strain; by approximating the compacted structure's volume with the beam material volume ($V_{compact}$) and by neglecting the Poisson's effects, the displacement at the compaction is:

(9) $\Delta H_{compact} = H - V_{compact}/A_{projection}$

where $A_{projection}$ is the area of projection of the structure on the horizontal plane. The estimation of compaction strains for each type of the structure and for cell size of 2,5mm, are 85%, 82% and 80%, respectively, for the investigated '*bcc*', '*bcc,z*' and '*$f_2$fcc,z*' configurations.

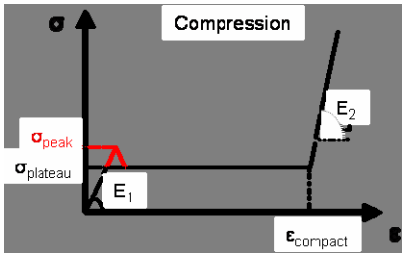

FIG 11. The basic design parameters of cellular core materials

The basic failure mechanism of the structure is plastic buckling instability, therefore both the geometrical and the material non-linearity, i.e. buckling and plasticity, contribute to the failure of the structure. Thus, for the simulation of static compression on the cellular structures, the initial geometric imperfection is introduced in the structure in the cases where the eigen-value buckling analysis indicates that the critical buckling load is less or equal to the failure loads measured in experiments. The results of the eigen-value buckling analyses and the measured failure loads for 2,5mm unit cell structures are given in TAB 4.

	bcc	bcc,z	$f_2$fcc,z
Eigen-value buckling critical load, MPa	8,5	1,76	6,095
Experimentally measured failure load, MPa	1	2,35	5
Initial geometric imperfection	no	yes	yes

TAB 3. Failure load measured from experiments and estimated by eigen-value buckling analysis

After introducing the initial geometric imperfection where required, a non-linear analysis including both material and geometric non-linearity is performed. The static compressive loading is introduced and the results in the form of 'global' engineering stress-strain data are compared to the experimental data of Ref. [22]. The comparison of experimental and numerical results is presented in FIG 12.

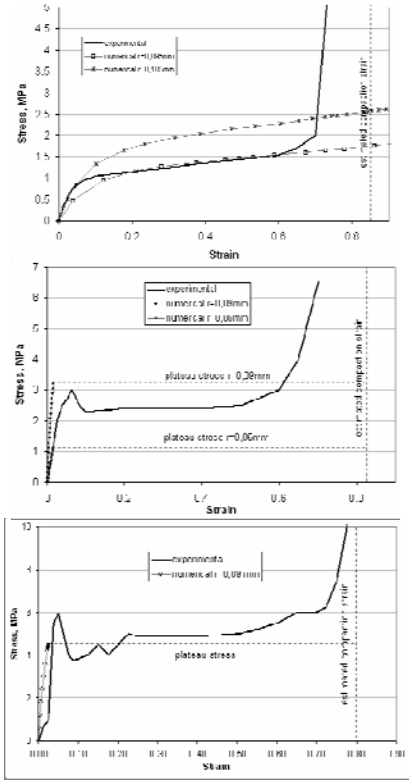

FIG 12. Comparison between experimental and numerical 'global' stress-strain curves for a) bcc, b) bcc,z and c) $f_2$fcc,z structures (cell size 2,5mm).

CONCLUSIONS

The structural behavior under impact loading for various crashworthiness structural types and material systems is analysed. Numerical analysis tools can have an essential contribution to the analysis. They can be used in the study of the energy absorption characteristics, the real crushing modes, the scaling effects between full-scale behavior and tested models and partly in the verification procedure. However, a careful selection of the numerical modeling parameters and sophisticated utilization of the capabilities of the numerical codes is required.

Concerning the high velocity bird-strike simulations, a numerical simulation methodology has been successfully developed to model the bird strike on an innovative Leading Edge design, based on the 'tensor skin' energy absorbing concept. The numerical simulation results are compared to experimental bird strike test data, leading to conclusions about the success of both the design concept and the simulation methodology.

The cellular core of a sandwich composite structure is analysed via a non-linear elastoplastic analysis including initial imperfections and geometrical non-linearity. Numerical results have shown that the structural response is strongly influenced by the unit cell geometrical and material properties.

All the developed simulation models may be considered as useful tools in the design, optimization and proof process of innovative crashworthiness concepts.

REFERENCES

[1] 1. S. Fenves, N. Perrone, A. Robinson, W. Schnobrich (1973). Numerical and Computer Methods in Structural Mechanics. Academic Press, NewYork , pp. 558-563.
[2] M.C.-Y Niu (1988). Airframe Structural Design. Conmilit Press Ltd.
[3] E. Haug, A. De Rouvray (1993). Crash Response of Composite Structures", Chapter 7 in "Structural Crashworthiness and Failure, Eds: Jones N, Wierzbicki T., Elsevier Science.
[4] L.W. Bark, J.D. Cronkhite, L.T. Burrows, L.M. Neri (1988). Crash Testing of Advanced Composite Energy Absorbing Repairable Cabi Subfloor Structure. American Helicopter Society Meeting, Virginia, October 23-27.
[5] H. Thuis, H. Vries, J. Wiggenraad. Subfloor skin panels for improved Crashworthiness of Helicopters, NLR-TP 95082 U.
[6] A. Obdam (1993). Composite tensors, concept evaluation, Internal Report, NLR (in Dutch).
[7] Michielsen A.L.P.J. and Wiggenraad J.F.M., "*Review of crashworthiness research of composite structure.*", NLR-CR 97046, 1997
[8] PAM-CRASH Users Manual, Engineering Systems International, 1997
[9] Ladevèze P, Le Dantec E. (1992). Damage Modelling of the elementary ply of laminated composites. Composites Science and Technology is. 43, pp.257-267.
[10] L.C. Ubels (1997). "Initial Material data, Crasurv Task 1.1", NLR-TR 97308L.
[11] Q. M Li, R. Mines, and R. S (1997). Initial Material data for Composite Materials, Univ. Liverpool, IRC/151/97.
[12] L.C. Ubels. Behavior of shear panels (1997). NLR-TR 97534
[13] D. Kohlgrueber, H. Weissinger (1997). D.4.1.3. Results of Dynamic Tests of Tensor Skin Panels, DLR-IB 435-97/31
[14] W. Lestari (1994). Crashworthiness Study of a Generic Composite Helicopter Subfloor Structure. NLR-TR 93590 L.
[15] Cook RD, Malkud DS, Plesha ME. (1989). Concepts and applications of finite elements analysis, Wiley.
[16] Swanson Analysis Systems, ANSYS Users Manual, Rev. 5.1,1996
[17] H. Thuis, J. Wiggenraad (1992). The influence of Trigger Mechanisms and Geometry on the Crush Characteristics of Sine Wave beams., NLR contract report CR 92133 C.
[18] Gallard, J. P., Report on Composite Commuter Leading Edge Bird Strike Tests, CRAHVI internal report, CEAT, 2002, p. 7.References
[19] Gibson, L. J. and Ashby, M. F., Cellular solids, Cambridge Solid State Science Series, Cambridge University Press, Cambridge, United Kingdom, 1997.
[20] Zenkert, D.A., Introduction to Sandwich Construction, EMAS Publishers, 2000.
[21] Mines, R.A.W, McKown, S., Cantwell, W., Brooks, W. and Sutcliffe, C. J., On the Progressive Collapse of Micro Lattice Structures, 13th International Conference on Experimental Mechanics, Alexandroupolis, Greece, 2007.
[22] McKown, S and Mines, R.A.W., Impact behaviour of metal foam cored sandwich beams, 16th European Conference on Fracture , Alexandroupolis, Greece, Paper No. 254, July 2006.
[23] Th. Kermanidis, G. Labeas, M. Sunaric and R. Ubels, 'Development and validation of a novel bird strike resistant composite leading edge structure'', in Applied Composite Materials, 12, pp. 327-353, 2005.
[24] G. Labeas and Th. Kermanidis**, '**Crushing behaviour of the Energy Absorbing 'Tensor Skin' panels', in Fatigue and Fracture of Engineering Materials and Structures, vol. 26, pp. 449-457, 2003.
[25] G. N. Labeas, M. Sunaric, 'Failure behaviour investigation of metallic open lattice cellular structures', in Proc. of the International Conference on Experimental Mechanics, pp. 161, July 1-6, 2007, Alexandroupolis, Greece, July 1-6, 2007